Fuel 116 (2014) 158–167

Contents lists available at ScienceDirect

Fuel

journal homepage: www.elsevier.com/locate/fuel

Integrated biomass torrefaction – Chemical looping combustion as a method to recover torrefaction volatiles energy

A. Sarvaramini, F. Larachi *

Department of Chemical Engineering, Laval University, Québec, QC G1V 0A6, Canada

HIGHLIGHTS

- Birch wood was torrefied between 260 and 300 °C in a fixed bed reactor.
- Chemical looping combustion of torrefaction volatiles over iron oxide was studied.
- Up to 99% of carbon released during torrefaction was converted to CO_2 at 600 °C.
- Presence of CO_2 and steam did not affect the properties of torrefaction products.

GRAPHICAL ABSTRACT

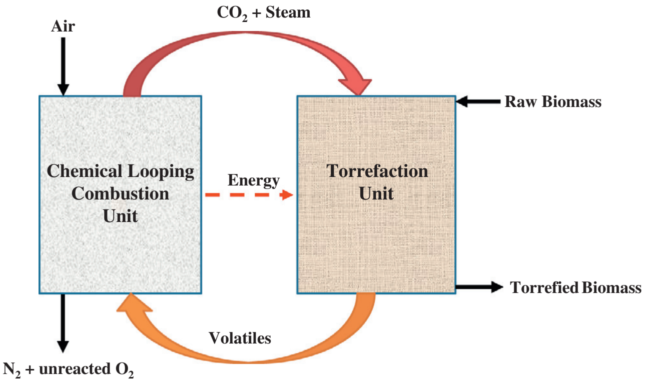

ARTICLE INFO

Article history:
Received 17 June 2013
Received in revised form 28 July 2013
Accepted 29 July 2013
Available online 15 August 2013

Keywords:
Biomass torrefaction
Chemical looping combustion
Iron oxide oxygen carrier
Volatiles composition
Burn-off of carbonaceous deposits

ABSTRACT

Hyphenation of biomass torrefaction to chemical looping combustion (CLC) was studied experimentally. The concept consists of burning the torrefaction volatiles using iron oxide as solid oxygen carrier whereby the CLC flue gas, mostly non-diluted CO_2 and steam, is recirculated to the torrefaction reactor for heat integration. Also, being deprived of nitrogen and oxygen, the CLC flue gas allows pure CO_2 to be recovered and further captured or sequestered thus setting a frame for a negative net CO_2 torrefaction in co-firing plants to reduce greenhouse gas emissions. Birch wood was torrefied between 260 and 300 °C and the resulting volatiles were burned over iron oxide solid oxygen carriers between 400 and 600 °C converting up to 99% of volatile carbon into CO_2. Oxygen carrier stability for burning torrefaction volatiles and oxygen depletion during CLC were assessed vis-à-vis deactivation, and CO and hydrogen production. Also, the buildup of CO_2 and water vapor in the recirculating torrefaction gas and their incidence on the properties of torrefied solid product were quantified in terms of mass and energy yields, equilibrium moisture content and grindability of the torrefied birch wood.

© 2013 Elsevier Ltd. All rights reserved.

1. Introduction

Coal combustion in the electricity generation plants is considered as one of the most important sources of greenhouse gas emission [1]. Replacing coal with biomass as a renewable CO_2-neutral energy source in energy conversion systems could be an option to reduce net CO_2 production [2]. However, raw biomass as a fuel features some drawbacks such as low calorific value due to its high moisture and oxygen contents [3,4], high grinding energy requirement due to its rigidity and mechanical strength [5,6], and low flowability and fluidization properties leading to difficulties in feeding it into boilers [7]. Improving these biomass properties via torrefaction is envisioned as a prerequisite step to adapt biomass properties to those of a fuel for efficient coal/biomass co-firing [7]. Torrefaction increases the energy density of biomass by reducing its oxygen content leading to a torrefied biomass product with heating values nearing those of coal [5,8,9].

---

* Corresponding author. Tel.: +1 418 656 3566; fax: +1 418 656 5993.
E-mail address: faical.larachi@gch.ulaval.ca (F. Larachi).

0016-2361/$ - see front matter © 2013 Elsevier Ltd. All rights reserved.
http://dx.doi.org/10.1016/j.fuel.2013.07.119

Furthermore, torrefaction promotes partial depolymerization/decomposition of cellulose and hemicellulose reducing the fibers length and mechanical stability and resulting in improved grinding properties [7,10,11].

Biomass torrefaction is performed at temperatures below 300 °C which prompts partial decomposition of hemicellulose, cellulose and lignin biomass constituents [7,12]. Decomposition is accompanied with the release of condensable and non-condensable volatiles such as CO_2, CO, CH_4, H_2O and some hydrocarbon oxygenates (acetic, formic and lactic acids) [13]. In the usual industrial torrefaction practices, the produced volatiles are burned with air in a combustion unit and the hot flue gas is routed toward the pre-drying and torrefaction segments to pick up directly or indirectly its heat content [14,15]. Ideally well-designed torrefaction processes are thermally self-sufficient. That is, if apart from the heat released from the combustion of the torrefaction gases, no additional energy make-up is necessary to ensure their operation [15]. Direct contact of flue gas with biomass during torrefaction could be an efficient way for the heat to transfer to the biomass. However, the presence of residual O_2 in the flue gas could lower the efficiency of biomass torrefaction by burning a fraction of the biomass itself [14,16]. Furthermore, air consisting overwhelmingly of inert N_2 results in the handling of large flue gas volumes which translate into increased investments in terms of piping and ancillary equipment [14,16].

In recent years, the concept of chemical looping combustion (CLC) has been widely studied as a promising alternative for fossil fuel combustion while preventing dilution issues of the flue gas [17–19]. In this concept, the required oxygen for fuel combustion into CO_2 and water is supplied by a solid oxygen carrier such that after oxidation a N_2-free flue gas is obtained. The concept is implemented in two interconnected reactors with one performing the fossil combustion/solid oxygen carrier reduction while in the other the solid carrier regeneration/oxidation by air takes place [17,18]. However in practice, both spatial [17,18] and temporal segmentations [20] are possible by enabling the solid oxygen carrier either to circulate between two reactors or exposed, in a stationary manner, to periodic oxidative/reductive cycles within the same reactor. The N_2-free flue gas leaving the combustion reactor could be further processed to remove water and the remaining CO_2 could be captured, sequestrated or used for other applications.

To the best of our knowledge, no work has been reported to evaluate whether integration of torrefaction with CLC of torrefaction volatiles is advantageous or not. In the present work the potential of this combination was studied. The gas evolved during torrefaction was routed to a CLC reactor in which the acid hydrocarbons, CO, CH_4 and H_2 are burned at the contact with a solid oxygen carrier and without oxygen gas. The CLC hot flue gas stream, consisting of CO_2 and water, or a fraction of it could be recycled to the upstream torrefaction unit to transfer heat for the torrefaction of the solid biomass particles. This concept is believed to have two main advantages over existing processes. First, the hot flue gas being O_2-deprived will present no risk of burning biomass during torrefaction. Second, preliminary condensation and separation of water from the CLC flue gas will lead to a pure CO_2 stream which could be capture via physical or chemical solvents in a conventional gas–liquid scrubber [21,22] or directly sequestrated in mining residues via dry or wet carbonation [23–25]. As biomass is CO_2-neutral energy source, a negative net CO_2 emission from torrefaction could be very appealing for mitigating CO_2 emissions in the atmosphere in the future bioenergy co-firing plants hyphenated with carbon capture and storage plants [26].

2. Experimental

2.1. Materials

Isothermal torrefaction studies were performed using birch, an abundant woody biomass sample from Québec forests. Before the experiments, the as received tiny sheets of birch wood samples were cut into small pieces to obtain woodchips in the size range of 2–4 mm. The proximate analysis of the birch wood showed the presence of 5.5% of humidity. The volatiles, fixed carbon and ash content of the samples were 89.4%, 9.8% and 0.7% on dry basis, respectively.

The oxygen carrier used in this study was an iron oxide powder prepared from pure iron metal powder (Atlantic Equipment Engineering, AEE) with 99.9% purity and particle size <149 μm. Iron oxide is considered as an inexpensive and environmentally safe compared to the other solid oxygen carriers such as nickel and cobalt oxides [27]. Prior to experiments, the iron powder samples were calcined in air for 3 h at 600 °C to form oxide particles.

2.2. Experimental setup

The schematic diagram of the experimental assembly is shown in Fig. 1. The experimental setup mainly consists of two connected torrefaction and chemical looping combustion reactors. Birch wood torrefaction was performed in a stainless steel tube (ID. 34 mm, length 70 cm) placed inside an induction coil while the samples were held atop of a steel grid located in the tube's middle. The torrefaction temperature was controlled by a fiber optic pyrometer connected to a temperature controller to meter the induction-heater power. Temperature was also measured via a *K* type thermocouple inserted in the center of the biomass layer. The difference in temperatures between the bed and the tube surface never exceeded 5 °C in steady-state conditions. The gas exiting the torrefaction tube was transferred to a CLC stainless steel tube (ID. 10 mm, length 40 cm) from the top via a heated tube preventing volatiles condensation during transit. This latter was located in a vertical electrically-heated furnace equipped with a PID temperature controller and a *K* type thermocouple for CLC temperature control. The combustion gas exiting the CLC reactor was sent to an ice water cold trap to separate the remaining volatiles from the gas before recirculating it to the torrefaction reactor. Before entering the torrefaction reactor, gas samples were analyzed using Agilent micro GC 3000 for their CO, CH_4, H_2 and CO_2 composition.

The following procedure was applied for performing each simultaneous torrefaction and CLC experiment: initially 500 mg of birch wood and 10 g of iron oxide particles were loaded in the middle of torrefaction and CLC reactors, respectively. Next, the CLC reactor was heated to the desired temperature and kept there for 30 min to stabilize its temperature. Afterwards, the entire assembly was purged with N_2 (CO_2, or mixture thereof) at 1 L/min to get rid of remnant gaseous oxygen. After oxygen was below micro GC detection limit, gas recirculation in the torrefaction-CLC assembly was resumed and torrefaction reactor temperature was raised from ambient to either 260 °C or 300 °C and kept there for 60 and 20 min durations, respectively. The concentration of CO_2, CO, H_2 and CH_4 accumulated in the assembly was measured every 5–6 min using micro GC. In some of the experiments referred to as blank experiments the CLC reactor was bypassed and the volatiles released from the torrefaction reactor were headed directly to the cold trap without any further combustion in the CLC. These experiments were performed to investigate the accumulation of CO, CO_2, CH_4 and H_2 in the assembly during the birch wood torrefaction and in the absence of CLC.

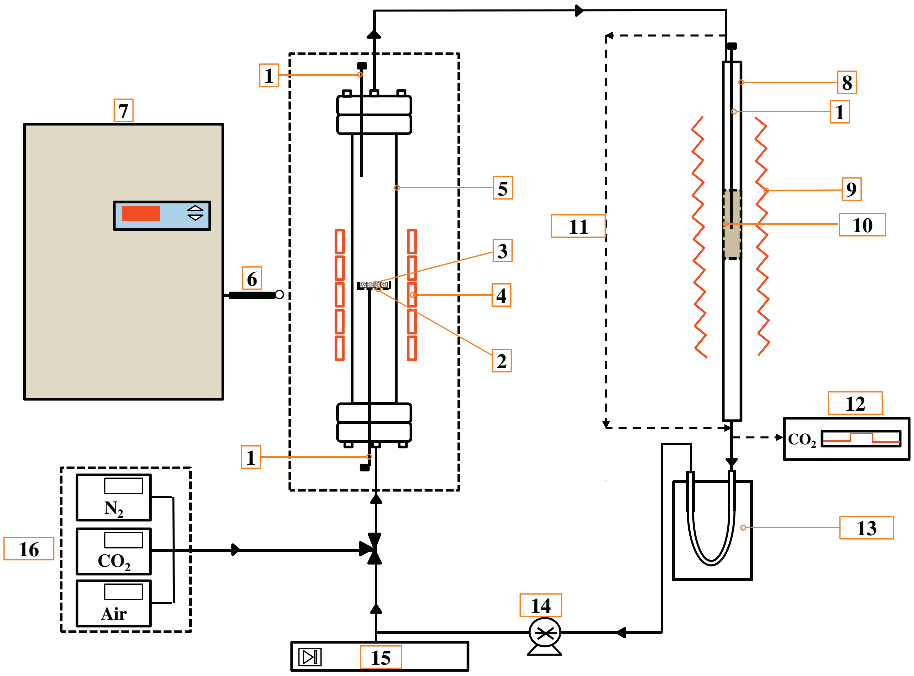

Fig. 1. The schematic of experimental torrefaction-chemical looping combustion assembly: (1) *K* type thermocouple, (2) stainless steel mesh, (3) birch sample, (4) induction coil, (5) stainless steel torrefaction reactor, (6) pyrometer, (7) induction heater power supply, (8) chemical looping combustion reactor, (9) electric heater, (10) iron/iron oxide fixed bed, (11) CLC shortcut line, (12) CO_2 infrared detector used during iron oxide regeneration, (13) cold trap, (14) peristaltic pump, (15) micro GC and (16) mass flow meters.

A regeneration cycle was started at the end of the test where the solid oxygen carrier was regenerated at 600 °C using oxygen (5% O_2 in N_2) as an oxidant to burn the carbon deposits that formed on the surface of iron oxide particles. CO_2 evolved during regeneration was monitored online using an infrared CO_2 detector to quantify the amount of deposited carbon in each combustion cycle. Finally, the dry torrefied birch wood was removed from the steel grid and then weighed to obtain its mass yield (Y_M = %mass solid product/mass feed). The C, H, N, S contents of the samples were obtained using an elemental analyzer (Fisons EA 1108CHNS). All measurements were repeated twice and their averages reported. The higher heating value (HHV) of the samples before and after torrefaction was determined using a relationshipobtained by Channiwala et al. [28] based on carbon, hydrogen, oxygen, sulfur, nitrogen and ash content of biomass. Using the solid product HHV, the energy density ratio (e = HHV solid product/HHV feed) and energy yield ($Y_e = e\ Y_M$) were also determined.

Acid acetic is an oxygenated hydrocarbons forming during biomass torrefaction [13,29]. Therefore, acetic acid was used as a model torrefaction volatile compound to assess the long-time stability for the combustion of torrefaction-formed volatiles and the possible effect of deactivation on the distribution of CLC gas products for the iron oxide oxygen carrier. Although acetic acid is only one of the constituents of torrefaction volatiles, use of acetic acid as a model torrefaction volatile for long-term stability tests has some advantages over the volatiles released from direct birch torrefaction. First, the concentration and flow rate of volatiles released from birch torrefaction could change with time while the concentration and flow rate of model acetic acid volatile was controlled leading to accurate conversion calculations over time for the assessment of the long-term stability tests. Second, the lack of oxygen on the solid oxygen carrier leads to the formation of some H_2, CO and CH_4 due to the cracking of volatiles. However, since torrefied biomass also releases some H_2, CO and CH_4, it is difficult to distinguish between these gases during biomass torrefaction or during the long-term stability test due to lack of oxygen on the solid carrier. Consequently for these series of experiments 100 mL/min N_2 stream was saturated with acetic acid vapors by bubbling it through a temperature-controlled acetic acid pool. During the combustion cycle, the acid-saturated stream was contacted with 10 g of pre-oxidized iron particles at 600 °C in the CLC reactor and the concentrations of CO_2, CO, H_2, CH_4, oxygen and acetic acid were monitored. Likewise, when the combustion activity of the oxygen carrier declined enough, the combustion cycle was switched to a regeneration cycle by sweeping 200 mL/min of oxidizing gas stream (5% O_2 in N_2) during which the concentrations of CO, CO_2 and O_2 were registered.

The properties of torrefied birch as affected by steam and CO_2 in the torrefaction reactor were compared by conducting birch torrefaction in a 80:20 (mol.%) CO_2:water mixture and under N_2 environment. These properties were the mass and energy yield, higher heating value, CHO content of torrefied samples, humidity uptake and grindability of torrefied samples. The humidity uptake of torrefied and raw birch samples was measured under various relative humidity environments. A total of six saturated salt solutions with different equilibrium humidity at 30 °C were prepared: 7.38% (KOH solution), 11.28% (LiCl solution), 43.17% (K_2CO_3 solution), 75.09% (NaCl solution), 83.62% (KCl solution) and 97.08% (K_2SO_4 solution) [30]. 100 mg of raw and torrefied birch samples, first dried in an oven at 105 °C, were placed in flasks containing aforementioned saturated salt solutions. The flasks were kept for one week in a temperature-controlled oven at 30 °C while the samples weight change due to humidity uptake was measured daily. Samples reached equilibrium after almost four days. Samples with >3270 μm initial size were loaded in the grinding chamber in a ball mill operated at 500 rpm speed with balls of 15 mm diameter to determine grindability of torrefied and raw samples. To ensure similar conditions for the different biomass samples, an equal volume of biomass was loaded in the milling chamber. The samples were ground for 30 min and the final samples obtained were sieved with a series of sieves of mesh sizes 3270, 2000, 850 and 355 μm.

3. Results and discussion

3.1. Torrefied solid produced in torrefaction-CLC closed assembly

Table 1 shows the results of elemental analysis, mass and energy yields and higher heating value of raw birch and torrefied birch samples at 260 °C and 300 °C for 60 min and 20 min. The mass yield of samples torrefied at 260 °C and 300 °C were, respectively, around 76% and 64%, reflecting enhanced torrefaction rates with increased temperature despite a correspondingly shortened contact time. Torrefaction increased considerably the carbon content in the torrefied birch at the expense of hydrogen and oxygen contents. This reflected in atom ratio reductions from H/C = 1.54 and O/C = 0.72 for birch to H/C = 1.38 and O/C = 0.62 for birch torrefied at 260 °C and to H/C = 1.33 and O/C = 0.58 for birch torrefied at 300 °C. The decrease in H/C and O/C ratios led to 7.3% and 10.2% increase in HHV of birch torrefied at 260 °C and 300 °C, respectively. Although torrefaction increases birch HHV, the energy yield of torrefied birch at 260 °C and 300 °C was 81.8% and 71.4%, respectively, in accordance with partial loss of biomass energy during torrefaction. Such energy yield loss of the resulting torrefied solid is attributed to the release of carbon and hydrogen during torrefaction. On a dry wood basis, birch torrefaction at 260 °C led to the respective release of 13.1% and 22.1% of total carbon and hydrogen in the form of condensable and non-condensable gases. These levels were boosted at 300 °C torrefaction to 24% and 34.8% for carbon and hydrogen, respectively.

3.2. Gases released in torrefaction-CLC closed assembly

Torrefaction of birch without circulating volatile gas through the CLC reactor was referred to as blank experiment which is represented with black diamond symbols in Figs. 2–5. These figures show that nearly 17.1% and 13.2% of total release carbon (obtained from subtraction of carbon content of each sample before and after torrefaction on a dry basis) was in the form of CO_2 (Fig. 2a and b), 7% and 6.5% as CO (Fig. 3a and b), virtually no hydrogen (Fig. 4a and b), and 0.3% and 0.2% as CH_4 (Fig. 5a and b), respectively, at 260 °C and 300 °C. Consequently, the balance of the released carbon from the torrefied birch wood at 260 °C and 300 °C, respectively, contributed 75% and 80% of the total released carbon in the form of condensable volatiles. Combustion of, and energy recovery from, the condensable volatiles is accompanied with production of CO_2. Fig. 2a and b shows the trends of CO_2 production and accumulation in the torrefaction-CLC assembly during the separate torrefaction of birch wood at 260 °C and 300 °C and further combustion of the volatiles at 400 °C, 500 °C and 600 °C in the CLC reactor. As can be seen, the CO_2 concentration in the assembly increased with time due to simultaneous production of CO_2 from the torrefaction section and the combustion of volatiles in the CLC section. The torrefaction of birch at 260 °C and 300 °C and further combustion of volatiles at 400 °C led to the conversion of 55.1% and 29.9% of total released carbon to CO_2, respectively. CO_2 levels reached correspondingly 94.5% (99.1%) and 82.5% (93.6%) of total released carbon at 500 °C (600 °C) combustion temperature. For the same CLC temperature, the extent of volatiles combustion was higher the lower the torrefaction temperature, although volatiles combustion increases conversion to CO_2 using iron oxide particles the higher the CLC temperature. Torrefaction of birch wood at 300 °C being much faster than at 260 °C was likely to produce some tar compounds [13] with more thermally stable structure than some acid oxygenated hydrocarbons such as acetic acid and formic acid known to be formed at low temperature torrefaction.

Figs. 3–5 show the respective trends of CO, H_2 and CH_4 production and accumulation in the torrefaction-CLC assembly as non-condensable gases produced during birch torrefaction. A large amount of CO was produced and accumulated during blank experiments contributing ca. 7% and 6.6% of total released carbon from the torrefied birch at 260 °C and 300 °C, respectively (Fig. 3a and b). The accumulated CO in the assembly slightly increased in the experiments performed with CLC reactor at 400 °C for the torrefied birch at 260 °C and 300 °C. The partial decomposition of volatiles across the CLC could produce some CO leading to the observed increase of CO concentration in the assembly. However, increasing CLC temperature to 500 °C considerably reduced the amount of CO accumulated in the assembly as it was oxidized into CO_2 through the iron oxide bed. At 600 °C, CO contributed less than 2% of total released carbon from the birch wood torrefied at 260 °C and 300 °C. The trend of H_2 production and accumulation in the assembly was somehow different from that of CO. Blank torrefaction at 260 °C was virtually exempt of H_2 production unlike at 300 °C whereby tiny H_2 amounts were formed. Also, the contacting of torrefaction volatiles with iron oxide at 400 °C produced small amounts of hydrogen (Fig. 4a) in accordance with the cracking of some volatiles in the CLC reactor. However, H_2 concentration declined with increased CLC temperature likely due to its oxidation to water (Fig. 4a and b). As a result, the accumulated H_2 in the assembly due to birch torrefaction at 300 °C was less than 0.23% of total released hydrogen atoms (obtained from subtraction of hydrogen content of each sample before and after torrefaction on a dry basis) from the torrefied biomass while no H_2 is observed in the assembly during the birch torrefaction at 260 °C and with the CLC performing at 500 °C and 600 °C. Unlike the low CH_4 production in blank torrefaction, contacting volatiles with iron oxide CLC bed led to an increase in methane composition in the torrefaction-CLC assembly. For instance at 600 °C, the amount of accumulated CH_4 was, respectively, 2.5% and 2.2% of total released carbon of birch torrefied at 260 °C and 300 °C. Even if CH_4 could form via volatiles cracking over iron oxide particles, activity of the latter was not sufficient to completely oxidize the produced methane.

At completion of each simultaneous torrefaction-CLC experiment, regeneration was performed to evaluate the amount of deposited carbon as well as to monitor oxygen consumption of the CLC reactor. Maximum carbon deposition was observed for CLC experiments performed at 500 °C. Torrefaction of birch at 260 °C and 300 °C and further combustion of their volatiles at 500 °C CLC temperature led to carbon deposition on the surface of iron oxide particles contributing ca. 3.4% and 2.6% of the total released carbon. The deposited carbon on the surface of iron oxide particles in the CLC reactor operating at 400 °C and 600 °C was less than 1.2%.

Five successive torrefaction/combustion cycles followed by oxide regenerations were performed to assess whether or not the activity of iron oxide particles for burning of volatiles was affected in the long run. Birch wood samples were torrefied at 260 °C for 1 h with CLC reactor operating at 600 °C. Fig. 6 shows the trends of CO_2

Table 1
Ultimate analysis, mass yield, higher heating value and energy yield of as received and torrefied birch.

Samples	C (wt%)	H (wt%)	N (wt%)	S (wt%)	O (wt%)	Ash (wt%)	Mass yield (Y_M, %)	Energy yield (Y_e, %)	HHV (kJ/g)
As received birch	47.6	6.1	0	0	45.6	0.7	……	100	18.7
Torrefied birch (260 °C, 60 min)	51.2	5.9	0	0	42.1	0.8	76.2	81.8	20.1
Torrefied birch (300 °C, 20 min)	52.7	5.8	0	0	40.7	0.8	64.8	71.8	20.6

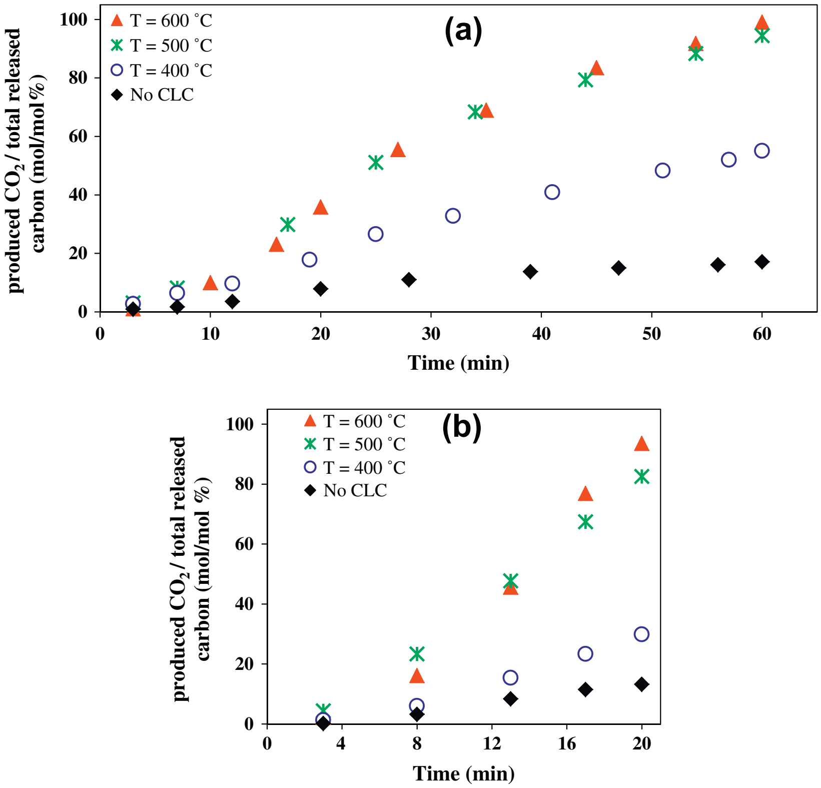

Fig. 2. CO_2 accumulation profiles during the torrefaction of 500 mg of birch at 260 °C (a) and 300 °C (b) for different combustion temperatures in the torrefaction-CLC assembly.

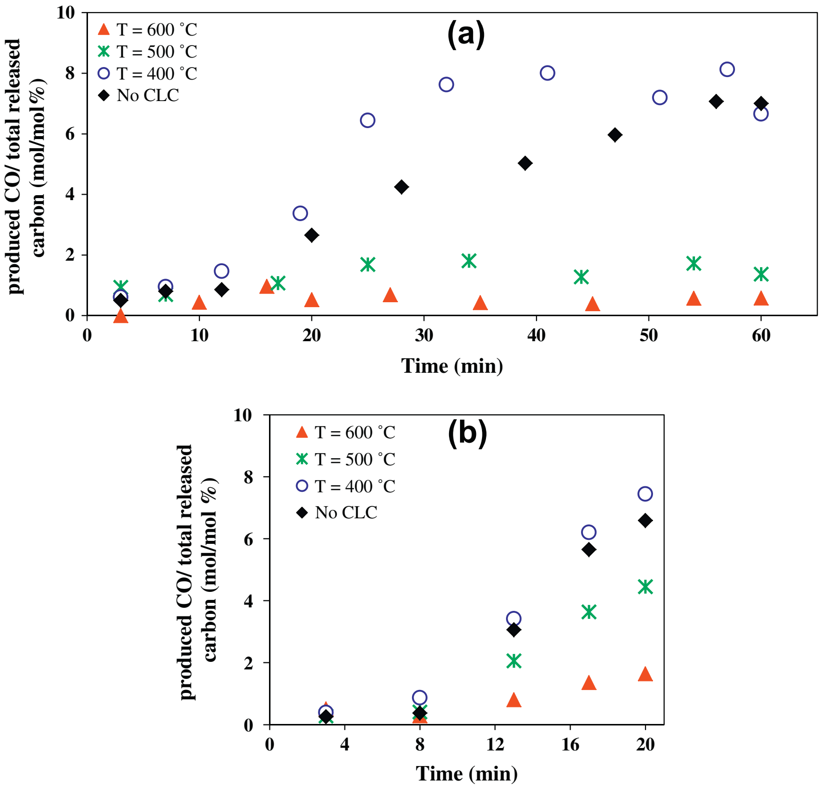

Fig. 3. CO accumulation profiles during the torrefaction of 500 mg of birch at 260 °C (a) and 300 °C (b) for different combustion temperatures in the torrefaction-CLC assembly.

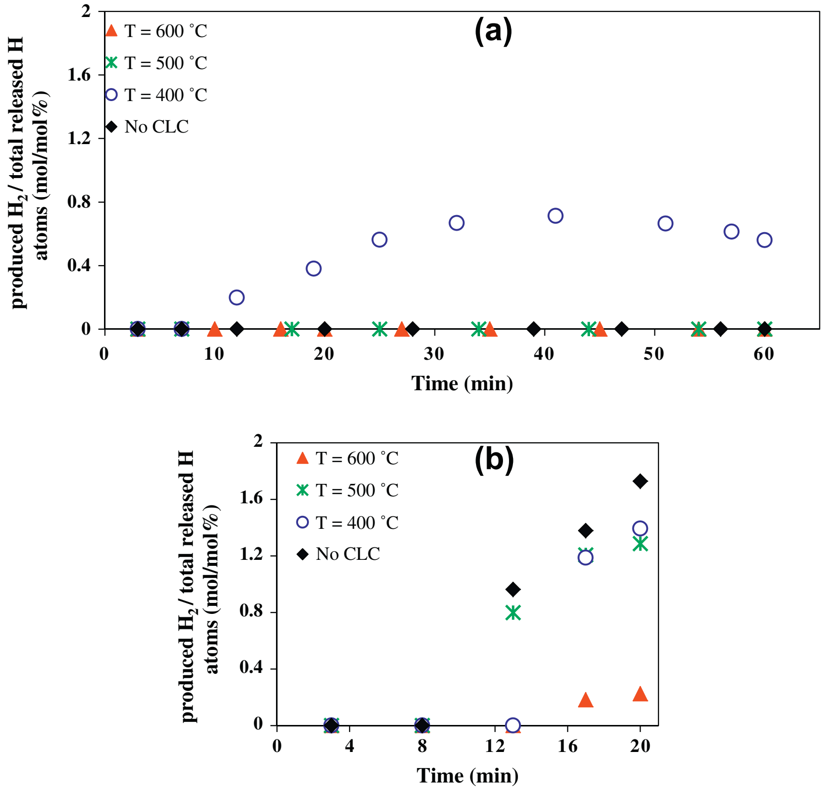

Fig. 4. H_2 accumulation profiles during the torrefaction of 500 mg of birch at 260 °C (a) and 300 °C (b) for different combustion temperatures in the torrefaction-CLC assembly.

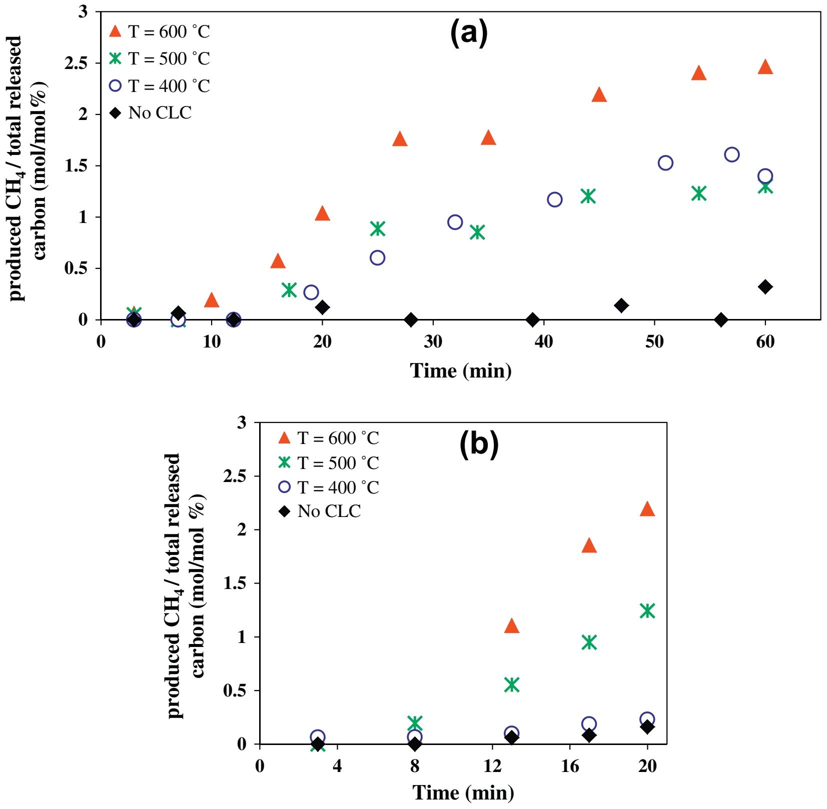

Fig. 5. CH_4 accumulation profiles during the torrefaction of 500 mg of birch at 260 °C (a) and 300 °C (b) for different combustion temperatures in the torrefaction-CLC assembly.

production and accumulation during simultaneous torrefaction and combustion as well as the oxygen concentration during the regeneration steps. CO_2 production and accumulation during the five cycles followed almost an identical pattern with no considerable decrease in iron oxide activity for combustion of volatiles in the CLC reactor.

To investigate if the presence of high CO_2 concentrations could influence the activity of iron oxide particles in the CLC reactor for the oxidation of volatiles, an experiment was performed with a mixture 50%:50% of CO_2 and N_2, 500 mg of birch wood sample torrefied at 260 °C for 1 h and 10 g of iron oxide oxygen carriers preheated and operated at 600 °C. The results showed that the presence of initial CO_2 did not affect the activity of iron oxide particles for combustion of volatiles. Almost 97.6% of the released carbon was found in the form of CO_2. No hydrogen and very small amount of methane were detected. The amount of accumulated CO in the assembly, slightly larger in the presence of CO_2, is easily rationalized in terms of reverse Boudouard reaction limiting oxidation of iron oxide particles and consequently resulting in the release of CO.

3.3. Long term stability

Product gas distribution during combustion in CLC reactor of model acetic acid is shown in Fig. 7a. During the first 90 min of acetic acid combustion through iron oxide oxygen carrier particles, CO_2 concentration was highest. Concomitantly, low CO and CH_4 concentrations were detectable while no residual acetic acid was detected at the CLC reactor outlet confirming complete acid conversion. Almost 97% of incident carbon was converted into CO_2 showing that the oxygen carrier function was active during this period. Later on, the exit CO_2 concentration began a decline while that of CO started to rise as did hydrogen though this latter went undetected before 90 min. Yet no acetic acid was observed in the exit stream. This indicates that acetic acid thermally cracked over the surface of iron oxide particles. However, due to oxygen lack, CO_2 and water production was hampered at the expense of CO and H_2 accumulation. Scrutiny of the carbon mass balance revealed that after 90 min, large amounts of carbon should have been deposited over iron oxide particles. Reduction in the formation of H_2, CO and CH_4, and carbon deposit correlates with reduction in the duration of CLC combustion and resumption of regeneration of the oxygen carriers. Fig. 7b illustrates the time evolution of oxygen, CO and CO_2 concentrations during oxidation. As can be seen, CO and CO_2 concentration peaks were observed upon switching CLC reactor into an O_2-containing feed. CO_2 and CO concentration showed that almost 11.1% of incident carbon introduced to the CLC reactor during the combustion period converted into carbon deposits on the oxygen carrier particles. Carbon deposition was mostly the result of fading activity of the oxygen carrier after 90 min combustion period. Oxygen concentration during the first 15 min of oxidation cycle was almost zero due to the burning of carbon deposits and oxidation of the oxygen carrier. However, after this time period the oxygen concentration increased progressively in the outlet gas, reaching a constant level indicative of completion of the oxidation step.

3.4. Effect of torrefaction environment on properties of torrefied solid product

Studies addressing the effect of torrefaction environment due to water vapor or CO_2 on the properties of torrefied solid products are to the best of our knowledge are very limited. Eseltine et al. [31]

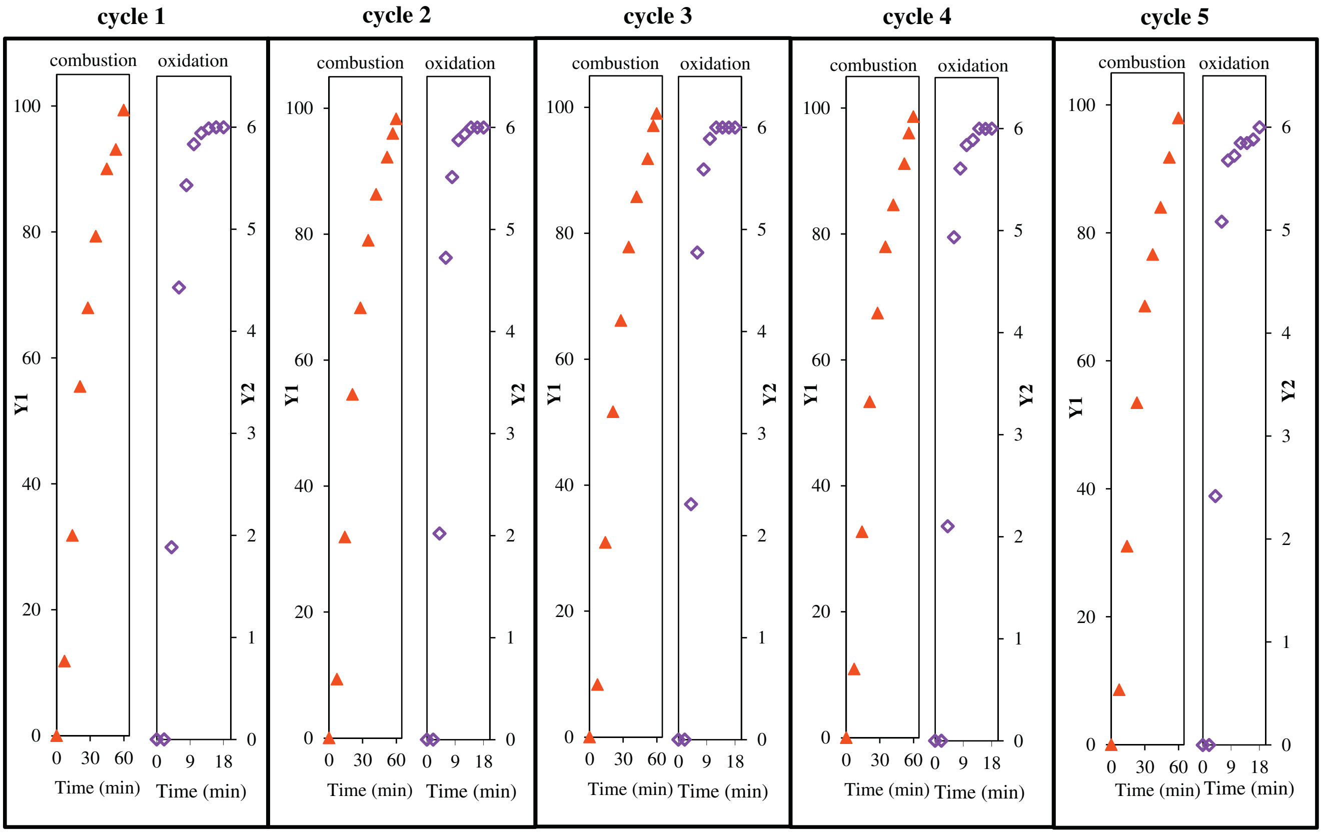

Fig. 6. Profile of CO_2 production and oxygen consumption during five cycles of torrefaction/combustion and oxidation/regeneration of iron oxides. Torrefaction and CLC temperatures were, respectively, 260 °C and 600 °C. Red triangle = % released carbon converted to CO_2. Purple diamond = O_2 concentration exiting CLC reactor during oxidation/regeneration. Initial O_2 concentration during oxidation was 6 mol% for N_2 flow-rate of 200 mL/min. Y_1 = produced CO_2/total released carbon (mol/mol%), Y_2 = oxygen concentration (mol%). (For interpretation of the references to color in this figure legend, the reader is referred to the web version of this article.)

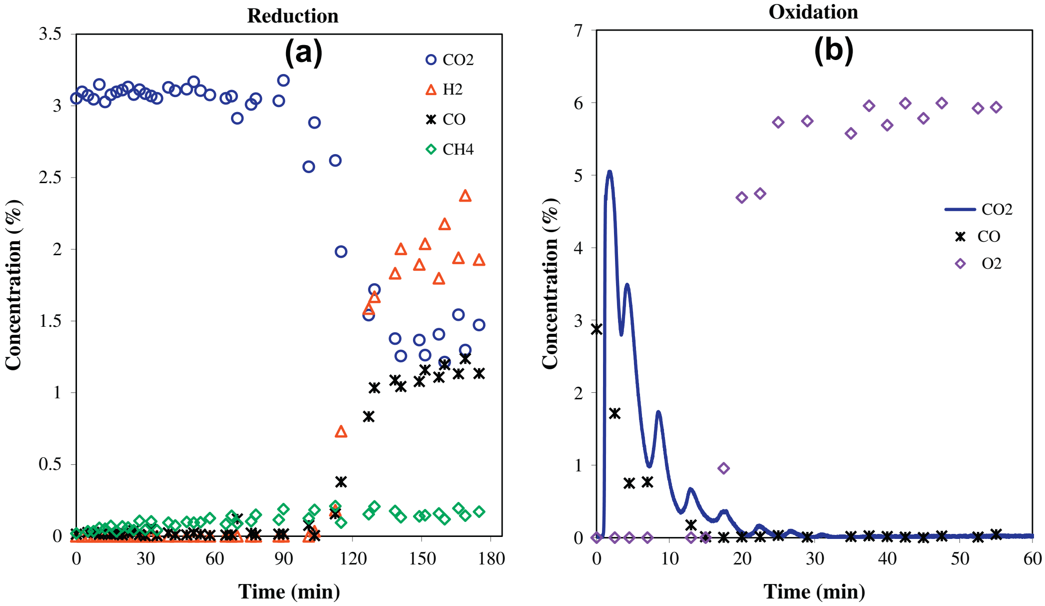

Fig. 7. Gas products' distribution as a function of time during the reduction and oxidation steps of iron oxide at 600 °C with acetic acid model torrefaction volatile. Acetic acid concentration during reduction was 1.6 mol.% and N_2 flow-rate was 100 mL/min, initial O_2 concentration during oxidation was 6 mol% and N_2 flow-rate was 200 mL/min.

investigated the torrefaction of juniper and Mesquite samples under N_2 and CO_2 atmospheres using thermogravimetric analyzer and the weight loss of their samples was higher under CO_2 than in a N_2 environment, and the difference in the weight loss of CO_2-torrefied biomass and N_2-torrefied biomass reached up to 4% at 300 °C. The presence of CO_2 and water in the torrefaction reactor on the weight loss and properties of solid birch samples is also studied in this work. Birch wood torrefaction was therefore carried out under pure N_2 and water/CO_2 (20%/80%) atmospheres at 260 °C for 60 min and 300 °C for 25 min. The torrefied product mass yield, energy yield, equilibrium moisture content (EMC) and grindability were determined for each condition. The elemental analysis results of the torrefied samples are summarized in Table 2. The mass yields of birch torrefied at 260 °C under N_2 and water/CO_2 environments were 75.6% and 76.6%, respectively. These decreased at 300 °C to 61% and 61.5%, respectively. The mass yields of torrefied birch appeared to be virtually unaffected by whether the torrefaction atmosphere was N_2 or water/CO_2 while the results by Eseltine et al. [31] showed higher weight loss of their biomass samples in CO_2 environment. We also performed several birch wood torrefaction experiments under CO_2 and N_2 atmospheres in the thermogravimetric (TG) analyzer to verify if the results obtained using the fixed bed reactor are supported by those performed in TG (which is more adequate system in terms of samples' temperature control and homogeneity). The experiments performed in TG were divided into torrefaction experiments performed at 300 °C for 25 min and experiments performed at 260 °C for 60 min under N_2 and CO_2 atmospheres. Each experiment is repeated twice to ensure repeatability. As seen in Fig. 8, regardless of whether CO_2 or N_2 atmospheres prevailed, the rate of birch torrefaction was barely affected. However, birch wood mass loss during torrefaction was slightly lower in the presence of CO_2 than N_2 which strengthens the trends of results obtained in the fixed bed tests. The effect of CO_2 on the rate of biomass torrefaction could be dependent on the type of biomass and ash content of the samples. For example, the juniper and Mesquite samples used by Eseltine et al. [31] exhibit higher amount of ash content than the birch sample used in this study. Furthermore, the hemicellulose, cellulose and lignin content of the samples could be different; especially the structure of hemicellulose could be species-dependent leading to the observed differences in the torrefaction rate of biomass in the two studies. Similarly, samples torrefied under water/CO_2 had slightly higher carbon content, HHV and energy yield than those torrefied in N_2 environment. It is plausible that torrefaction temperature being not high enough, reactions between CO_2 (or steam) and solid birch wood keep relatively slow whereby water and CO_2 are viewed as inert agents in birch wood torrefaction. As a matter of fact, temperatures as high as 600–800 °C would be required to trigger significant reactivity between CO_2, water and birch wood sample via the Boudouard water–gas reactions [32,33].

The dependence of EMC of the torrefied samples on relative humidity and thermal treatment is illustrated on Fig. 9. The samples EMC at each specific relative humidity are calculated as below:

$$\mathrm{EMC}\ (\%) = \frac{W_e - W_d}{W_e} * 100$$

where in this equation, W_e is the weight of birch wood at equilibrium at each specified humidity and W_d is the weight of dry sample. As can be observed in this figure, torrefaction considerably

Table 2
Ultimate analysis, mass yield, higher heating value and energy yield of torrefied birch at different residence time and temperatures and under N_2 and water/CO_2 atmospheres.

Sample	C (wt%)	H (wt%)	N (wt%)	S (wt%)	O (wt%)	Ash (wt%)	Mass yield (Y_M,%)	Energy yield (Y_e,%)	HHV (kJ/g)
Torrefied birch (260 °C, N_2 , 60 min)	51.5	5.9	0	0	41.9	0.7	75.6	81.5	20.2
Torrefied birch (300 °C, N_2, 25 min)	53.7	5.8	0	0	39.6	0.9	61.0	68.6	21.1
Torrefied birch (260 °C, water/CO_2, 60 min)	51.7	5.9	0	0	41.6	0.8	76.6	83.3	20.4
Torrefied birch (300 °C, water/CO_2, 25 min)	54.2	5.8	0	0	39.1	0.9	61.5	69.8	21.3

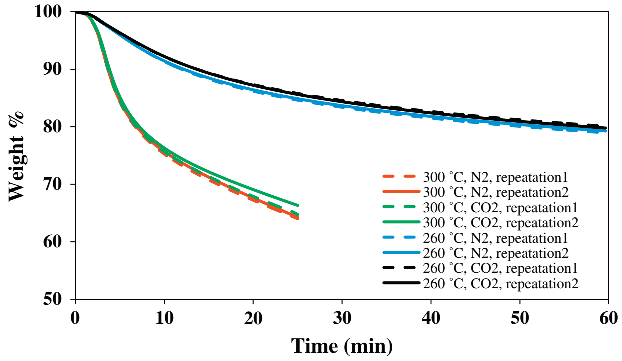

Fig. 8. Mass yield of birch wood torrefied at 260 °C and 300 °C in a thermogravimetric analyzer and under N_2 and CO_2 atmospheres.

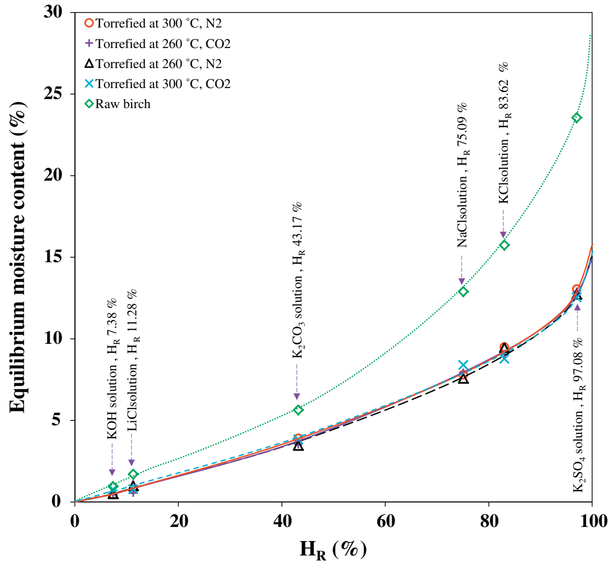

Fig. 9. EMC of raw and torrefied birch under water/CO_2 and N_2 environments. The relative humidity (H_R) prevailing for each salt solution is shown on *x*-axis, lines show trends.

decreased EMC of the torrefied samples as compared to raw birch whichever the prevailing relative humidity, H_R. EMC of torrefied birch under N_2 and water/CO_2 at $H_R = 97.1\%$ was ca. 45% less than that of non-treated birch emphasizing the considerable impact of thermal treatment on reducing wood humidity uptake. However, the EMC of the four torrefied samples at 260 °C and 300 °C in the water/CO_2 and N_2 environments at different relative humidity were very close to each other. Although the samples torrefied at 300 °C had smaller mass yield than those torrefied at 260 °C, the results show that the extent of birch torrefaction at 260 °C was enough to remove ample amounts of polar hydroxyl and carboxyl groups and yield similar moisture uptake patterns. The removal of hydroxyl and carboxyl groups of biomass during torrefaction reduces considerably the amount of bonded water in the biomass structure. Fig. 9 shows that at $H_R < 43.2\%$, the EMC of torrefied and raw samples increases almost linearly with increasing relative humidity. At low relative humidity, the dominant mechanism of water uptake in the biomass is adsorption through formation of strong bonds to the biomass network leading to the formation of bonded water [34]. However by increasing the relative humidity especially at $H_R > 90\%$, capillary condensation leads to the formation of some non-bonded water in the biomass cavities [35] leading to the exponential shape increase in the humidity uptake by increasing relative humidity (Fig. 9). Acharjee et al. [34] investigated the effect of thermal pretreatment on equilibrium moisture content of Loblolly pine and they concluded that the content of non-bonded water is independent of thermal treatment.

Fig. 10 shows the sieved particle size distribution of raw and torrefied birch samples at 260 °C and 300 °C and under N_2 and water/CO_2 environments after milling. Obviously, torrefied birch samples exhibit quite different size distribution than raw birch. Almost 90% of raw birch after 30 min milling did not pass the largest mesh size (3270 μm). The rigidity and mechanical strength of the biomass structure is attributed to the long crystalline cellulose fibers linked through the non-crystalline hemicellulose which results in its higher grinding energy requirement [5]. Torrefied birch samples, on the contrary, offered superior grindability by showcasing lesser mechanical strength and were more fragile as evidenced by the large proportions of fines after sieving. More than 25.7% and 28.8% of the ground birch wood torrefied at 260 °C for 60 min in N_2 and CO_2/water atmospheres, respectively, passed

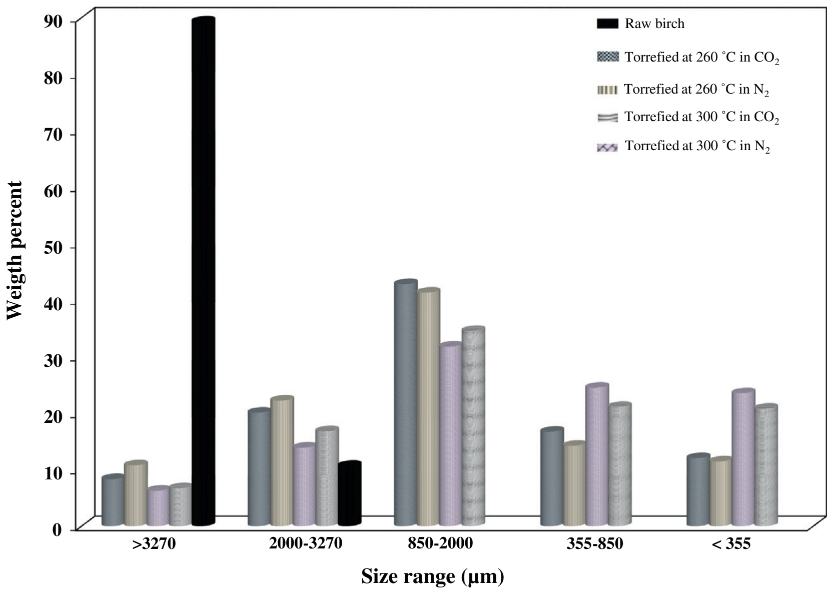

Fig. 10. Weight-based particle size distribution of ground raw and torrefied birch under water/CO_2 and N_2 environments.

the 850 μm sieve, whereas those for torrefied birch at 300 °C for 25 min were 48% and 42%, respectively, showing that the samples torrefied at 300 °C have better grinding properties than those torrefied at 260 °C. The partial depolymerization/decomposition of cellulose and hemicellulose during torrefaction reduces the fibers length and mechanical stability of biomass and as a result improves its grinding properties [7,10,11]. Although grindability of torrefied birch at 260 °C and under CO_2/water was slightly better than that under N_2 environment, this trend was not observed for the torrefied birch at 300 °C and the grindability of the torrefied birch under N_2 atmosphere was superior to that under CO_2/water environment.

4. Conclusion

A new concept of biomass torrefaction and volatile combustion in a chemical looping combustion (CLC) reactor using iron oxide particles was examined in this study. Birch wood as model biomass sample was torrefied in a fixed bed reactor at 260 °C and 300 °C and the volatiles resulting from torrefaction were burned over iron oxide solid oxygen carriers in a CLC reactor. Different CLC temperatures were tested and up to 99% of the carbon released during birch torrefaction was found in the form of CO_2 at 600 °C. The long-time stability of iron oxide particles for burning the torrefaction volatiles was investigated using acetic acid as a model volatile compound of biomass torrefaction. The lack of oxygen on the solid oxygen carrier could lead to the production of considerable amounts of CO and H_2 and also deposition of deactivating carbon on the surface of iron oxides. Examination of the effect of CO_2 and water in the torrefaction atmosphere on the properties of torrefied solid product revealed that these agents could increase slightly the HHV and energy yield of torrefied birch wood while they had no considerable effect on the mass yield and equilibrium moisture content of the obtained solid.

Acknowledgments

Support from the Natural Sciences and Engineering Research Council of Canada, the Canada Research Chair "Green processes for cleaner and sustainable energy", and the FQRNT-funded "Center in Green Chemistry & Catalysis" (CGCC) is gratefully acknowledged.

References

[1] Roy J, Sarkar P, Biswas S, Choudhury A. Predictive equations for CO_2 emission factors for coal combustion, their applicability in a thermal power plant and subsequent assessment of uncertainty in CO_2 estimation. Fuel 2009;88:792–8.
[2] McIlveen-Wright DR, Huang Y, Rezvani S, Mondol JD, Redpath D, Anderson M, et al. A techno-economic assessment of the reduction of carbon dioxide emissions through the use of biomass co-combustion. Fuel 2011;90:11–8.
[3] Chen WH, Kuo PC. Torrefaction and co-torrefaction characterization of hemicellulose, cellulose and lignin as well as torrefaction of some basic constituents in biomass. Energy 2011;36:803–11.
[4] Pimchuai A, Dutta A, Basu P. Torrefaction of agriculture residue to enhance combustible properties. Energy Fuels 2010;24:4638–45.
[5] van der Stelt MJC, Gerhauser H, Kiel JHA, Ptasinski KJ. Biomass upgrading by torrefaction for the production of biofuels: a review. Biomass Bioenergy 2011;35:3748–62.
[6] Ohliger A, Forster M, Kneer R. Torrefaction of beechwood: a parametric study including heat of reaction and grindability. Fuel 2013;104:607–13.
[7] Li J, Brzdekiewicz A, Yang WH, Blasiak W. Co-firing based on biomass torrefaction in a pulverized coal boiler with aim of 100% fuel switching. Appl Energy 2012;99:344–54.
[8] Medic D, Darr M, Shah A, Potter B, Zimmerman J. Effects of torrefaction process parameters on biomass feedstock upgrading. Fuel 2012;91:147–54.
[9] Sarvaramini A, Gravel O, Larachi F. Torrefaction of ionic-liquid impregnated lignocellulosic biomass and its comparison to dry torrefaction. Fuel 2013;103:814–26.
[10] Phanphanich M, Mani S. Impact of torrefaction on the grindability and fuel characteristics of forest biomass. Bioresour Technol 2011;102:1246–53.
[11] Repellin V, Govin A, Rolland M, Guyonnet R. Energy requirement for fine grinding of torrefied wood. Biomass Bioenergy 2010;34:923–30.
[12] Bridgeman TG, Jones JM, Shield I, Williams PT. Torrefaction of reed canary grass, wheat straw and willow to enhance solid fuel qualities and combustion properties. Fuel 2008;87:844–56.
[13] Prins MJ, Ptasinski KJ, Janssen F. Torrefaction of wood – Part 2. Analysis of products. J Anal Appl Pyrolysis 2006;77:35–40.
[14] Koppejan J, Sokhansanj S, Melin S, Madrali S. Status overview of torrefaction technologies. IEA bioenergy task 32 report. December, 2012.
[15] Uslu A, Faaij APC, Bergman PCA. Pre-treatment technologies, and their effect on international bioenergy supply chain logistics. Techno-economic evaluation of torrefaction, fast pyrolysis and pelletisation. Energy 2008;33:1206–23.
[16] CPK. Overview of international development in torrefaction. Kema report. <www.kema.com> 2011.
[17] Hossain MM, de Lasa HI. Chemical-looping combustion (CLC) for inherent CO_2 separations-a review. Chem Eng Sci 2008;63:4433–51.
[18] Adanez J, Abad A, Garcia-Labiano F, Gayan P, de Diego LF. Progress in chemical-looping combustion and reforming technologies. Prog Energy Combust Sci 2012;38:215–82.
[19] Moldenhauer P, Ryden M, Lyngfelt A. Testing of minerals and industrial by-products as oxygen carriers for chemical-looping combustion in a circulating fluidized-bed 300 W laboratory reactor. Fuel 2012;93:351–63.
[20] Iliuta I, Leclerc A, Larachi F. Allothermal steam gasification of biomass in cyclic multi-compartment bubbling fluidized-bed gasifier/combustor – new reactor concept. Bioresour Technol 2010;101:3194–208.
[21] Gazzani M, Macchi E, Manzolini G. CO_2 capture in integrated gasification combined cycle with SEWGS – Part A: Thermodynamic performances. Fuel 2013;105:206–19.
[22] Hasib-ur-Rahman M, Larachi F. CO_2 capture in alkanolamine-RTIL blends via carbamate crystallization: route to efficient regeneration. Environ Sci Technol 2012;46:11443–50.
[23] Assima GP, Larachi F, Beaudoin G, Molson J. CO_2 sequestration in chrysotile mining residues-implication of watering and passivation under environmental conditions. Ind Eng Chem Res 2012;51:8726–34.
[24] Assima GP, Larachi F, Beaudoin G, Molson J. Dynamics of carbon dioxide uptake in chrysotile mining residues – effect of mineralogy and liquid saturation. Int J Green Gas Control 2013;12:124–35.
[25] Pronost J, Beaudoin G, Tremblay J, Larachi F, Duchesne J, Hebert R, et al. Carbon sequestration kinetic and storage capacity of ultramafic mining waste. Environ Sci Technol 2011;45:9413–20.
[26] Milne JL, Field CB. Assesment report from the GCEP workshop on energy supply with negative carbon emissions, 2012.
[27] Abad A, Mattisson T, Lyngfelt A, Johansson M. The use of iron oxide as oxygen carrier in a chemical-looping reactor. Fuel 2007;86:1021–35.
[28] Channiwala SA, Parikh PP. A unified correlation for estimating HHV of solid, liquid and gaseous fuels. Fuel 2002;81:1051–63.
[29] Boateng AA, Mullen CA. Fast pyrolysis of biomass thermally pretreated by torrefaction. J Anal Appl Pyrolysis 2013;100:95–102.
[30] Greenspan L. Humidity fixed-points of binary saturated aqueous-solutions. J Res Natl Bureau Standards Sect A – Phys Chem 1977;81:89–96.
[31] Eseltine D, Sankar Thanapal S, Annamalai K, Ranjan D. Torrefaction of woody biomass (Juniper and Mesquite) using inert and non-inert gases. Fuel 2013;113:379–88.
[32] Khalil R, Varhegyi G, Jaschke S, Gronli MG, Hustad J. CO_2 gasification of biomass chars: a kinetic study. Energy Fuels 2009;23:94–100.
[33] Moon J, Lee J, Lee U, Hwang J. Transient behavior of devolatilization and char reaction during steam gasification of biomass. Bioresour Technol 2013;133:429–36.
[34] Acharjee TC, Coronella CJ, Vasquez VR. Effect of thermal pretreatment on equilibrium moisture content of lignocellulosic biomass. Bioresour Technol 2011;102:4849–54.
[35] Venkateswaran A. Sorption of aqueous and nonaqueous media by wood and cellulose. Chem Rev 1970;70:619–37.